ELSEVIER

Journal of Nuclear Materials 298 (2001) 1–10

journal of nuclear materials

www.elsevier.com/locate/jnucmat

Role and properties of the gel formed during nuclear glass alteration: importance of gel formation conditions

S. Gin *, I. Ribet, M. Couillard

Commissariat à l'Énergie Atomique (CEA/Valrhô), DRRV/SCD, B.P. 171, Bagnols-sur-Cèze cedex 30207, France

Abstract

A French SON 68 nuclear glass sample was experimentally altered to assess the mechanisms limiting the glass alteration kinetics, especially during the transition phase between the initial rate r_0 and the final rate under silicon saturation conditions. A glass specimen was altered at the initial rate for one week to form a silicon-depleted non-protective gel; the specimen was then leached under static conditions at a glass-surface-to-solution-volume (S/V) ratio of 500 m^{-1} and the alteration kinetics were compared with those of a pristine glass specimen altered under the same conditions. Unexpectedly, after static leaching the previously leached glass was 2.7 times as altered as the pristine specimen, and the steady-state silicon concentration was twice as high for the previously leached specimen. STEM characterization of the alteration films showed that the initial non-protective gel constituted a silicon pump with respect to the glass, and that the glass alteration kinetics were limited only when a fraction of the gel became saturated with silicon, and exhibited protective properties. This work also shows that silicon recondensation was uniform at micrometer scale: the silicon hydrolyzed at the reaction interface then diffused before recondensing over a length comparable to the gel thickness. In addition to these findings, this investigation suggests a reinterpretation of the effect of the S/V ratio on the glass alteration kinetics and on the steady-state dissolved silicon concentration. © 2001 Elsevier Science B.V. All rights reserved.

1. Introduction

The methodology for assessing the long-term behavior of a nuclear glass is based on modeling its alteration kinetics in the projected environment [1], i.e. taking into account the major factors affecting its behavior: temperature, ability of the environment to supply or remove kinetically limiting elements (e.g. silicon), flow rate, pH, solution composition, radioactivity, etc.

The alteration kinetics of borosilicate nuclear glasses are controlled by numerous concurrent mechanisms, including ion exchange between alkali metals (network modifiers) and protons in solution, hydrolysis of covalent bonds in the matrix, condensation of aqueous species at the reaction interface, and precipitation of secondary phases [2]. The importance of these mechanisms in the overall alteration process depends on the degree of reaction progress and on the alteration conditions. Initially, interdiffusion results in depletion of the alkali cations from the glass, causing the solution pH to rise [3]. When the thickness of the interdiffusion zone becomes constant, the glass alteration kinetics are controlled by surface reactions [4]. As long as the solution concentration remains relatively low, glass dissolution is congruent and the glass dissolves at its initial rate r_0, which depends only on the temperature and pH. As the reaction progresses and the solution becomes increasingly concentrated, the glass alteration kinetics generally diminish several orders of magnitude below r_0 [2].

The leaching behavior of French SON 68 (R7T7-type) nuclear glass has been widely studied since the early 1980s. The principal cause for the diminishing alteration rate of this glass has been attributed to the gel that develops at the interface between the pristine glass and solution [5–10]. Using different approaches, these authors have shown that solution saturation alone – notably with respect to silicon – is not sufficient to

---

* Corresponding author. Tel.: +33-4 66 79 14 65; fax: +33-4 66 79 66 20.

E-mail address: stephane.gin@cea.fr (S. Gin).

0022-3115/01/$ - see front matter © 2001 Elsevier Science B.V. All rights reserved.
PII: S0022-3115(01)00573-6

obtain low alteration rates. The gel arises from hydrolysis and condensation of silica species from the glass [2,11]. The development of a protective gel layer at the glass/solution interface forms a diffusion barrier that limits exchange phenomena. It has also been established that the presence in the gel of elements with high coordination numbers (e.g. zirconium or the rare earth elements) enhances the protective properties of the gel by favoring cross-linking [12]. The characteristic pore dimension in a protective gel is of the order of a nanometer [13]. The gel also tends to retain the actinide elements by sorption and coprecipitation, and thus appreciably enhances the glass containment properties with regard to long-lived radionuclides [14,15]. Allowance for the gel properties has become a major issue in assessing nuclear glass performance in France.

The degree to which the transport properties in the gel are affected by the pH, the temperature, or the silicon removal capacity of the environment remains unclear. In the mid-1980s, Chick and Pederson [16] concluded on the basis of a single experiment that the gels formed by nuclear glass alteration were non-protective. In reality the situation is more complex, and this conclusion cannot be generalized.

In order to understand the mechanisms responsible for the diffusion-limiting properties of a protective gel, we conducted an experiment in which a glass specimen was first altered at its initial rate for one week under flowing conditions, then placed in static conditions to study its alteration kinetics. The open-system alteration conditions resulted in the development of a thick non-protective gel layer. The alteration kinetics of this previously altered specimen were compared with those of a pristine glass specimen altered under the same static conditions. The alteration films formed during these tests were examined by transmission electron microscopy to determine the mechanisms involved. The alteration kinetics could be expected to be identical for both specimens, as the gel formed under initial rate conditions is non-protective.

2. Materials and methods

2.1. Glass fabrication and specimen preparation

Non-radioactive SON 68 glass [17], an R7T7-type nuclear glass with the composition detailed in Table 1, was tested as a powder, using the 160–250 μm size fraction with a specific surface area of 264 ± 15 $cm^2\ g^{-1}$ as determined by the BET (Kr adsorption) method. The powder was prepared by grinding and sieving monolithic glass blocks, then cleaned ultrasonically in acetone followed by alcohol and finally deionized water. The powder was dried and stored in a desiccator. Monolithic test coupons measuring $25 \times 25 \times 2.5\ mm^3$ were also cut from a larger glass bar, polished with SiC paper, and cleaned in the same way as the powder specimens.

Table 1
SON 68 (R7T7-type) glass composition

Oxide	wt%	Element	wt%
SiO_2	45.48	Si	21.26
Al_2O_3	4.91	Al	2.60
B_2O_3	14.02	B	4.35
Na_2O	9.86	Na	7.31
CaO	4.04	Ca	2.89
Li_2O	1.98	Li	0.92
ZnO	2.50	Zn	2.01
ZrO_2	2.65	Zr	1.96
Fe_2O_3	2.91	Fe	2.04
NiO	0.74	Ni	0.58
Cr_2O_3	0.51	Cr	0.35
P_2O_5	0.28	P	0.22
UO_2	0.52	U	0.46
ThO_2	0.33	Th	0.29
SrO	0.33	Sr	0.28
Y_2O_3	0.20	Y	0.16
MoO_3	1.70	Mo	1.13
MnO_2	0.72	Mn	0.46
CoO	0.12	Co	0.09
Ag_2O	0.03	Ag	0.03
CdO	0.03	Cd	0.03
SnO_2	0.02	Sn	0.02
Sb_2O_3	0.01	Sb	0.01
TeO_2	0.23	Te	0.18
Cs_2O	1.42	Cs	1.34
BaO	0.60	Ba	0.54
La_2O_3	0.90	La	0.77
Ce_2O_3	0.93	Ce	0.79
Pr_2O_3	0.44	Pr	0.38
Nd_2O_3	1.59	Nd	1.36
		O	45.21

2.2. Experimental procedure

The experiment was performed in two steps. A glass powder specimen (160–250 μm) was altered in pure water for 7 days under flowing conditions. The glass-surface-area-to-solution-volume (S/V) ratio was maintained at 50 m^{-1} and the flow rate at 1.3 ml min^{-1}, corresponding to a solution renewal rate of 1.87 d^{-1}. The test reactor was a 1-l Savillex PTFE container provided with a magnetic stirrer to agitate the solution without placing the powder in suspension. Two $25 \times 25 \times 2.5\ mm^3$ glass monoliths wrapped in Teflon gauze (70 μm mesh) were also suspended from a PTFE strip at mid-height in the reactor. The reactor was placed in a temperature-controlled chamber regulated at 90 ± 1°C. Solution samples were taken at the reactor outlet at regular intervals during the 7-day test; each sample was filtered to 0.45 μm at the test temperature, then acidified by an equivalent volume of 1 N nitric acid.

The pH was measured at the test temperature at each sampling interval. After 7 days of leaching under these conditions, one monolith was removed from the reactor, rinsed in deionized water, dried for 1 day at 50°C then weighed to estimate its mass loss and stored in a desiccator.

The altered glass powder and the second monolith were placed in a 120 ml PTFE reactor with 100 ml of water preheated to 90°C; the S/V ratio was 500 m^{-1}. In order to prevent any chemical or structural changes in the gel, the altered powder was neither dried nor cooled during the transfer. The reactor and its stirring system were placed in a temperature-controlled chamber regulated at 90 ± 1°C. One-milliliter solution samples were taken with a syringe at the following intervals: 1, 7, 14, 28, 56 and 84 days. Each sample was filtered to 0.45 μm at the test temperature, then acidified by an equivalent volume of 1 N nitric acid. The 84-day sample was taken in duplicate to detect the presence of any colloidal particles; the second sample was ultrafiltered to 10 000 Dalton by centrifuging at 4500 rpm, then acidified by an equivalent volume of 1 N nitric acid. The pH was measured at the test temperature at each sampling interval. On completion of the static test, the monolithic coupon was removed from the reactor, rinsed in deionized water, dried for 1 day at 50°C, then weighed to estimate its mass loss and stored in a desiccator.

In parallel with this static test on a previously altered glass specimen, an identical test was conducted with a pristine glass specimen. It also included a monolithic test coupon reserved for electron microscopic observation of the alteration products. The static test on previously altered glass is designated ST1, and the test with a pristine glass specimen ST2.

2.3. Solution analysis

The solution was analyzed by ICP-AES for Si, B, Na, Li, Al and Ca (with approximately 3% uncertainty).

2.4. Interpretation of results

The following parameters were calculated from the solution analysis results:

Normalized glass mass loss. After correcting the concentrations for acid dilution, the normalized mass losses were calculated from the following relation:

$$\mathrm{NL}_i = \frac{C_i}{X_i \cdot S/V}, \tag{1}$$

where C_i is the concentration (mg l^{-1}) of element i in solution, S/V is the glass-surface-area-to-solution-volume ratio (m^{-1}) and X_i the mass fraction of element i in the glass; the result is expressed in g m^{-2}. The normalized mass loss is used to assess the quantity of altered glass when calculated for the mobile elements (B, Na), as well as the retention capacity for less mobile elements (notably Si) in the alteration products.

Retention factor of element i in the alteration film. The retention factor f_i of element i in the glass alteration products is defined using boron as a glass corrosion tracer [18] according to the following relation:

$$f_i = \frac{\mathrm{NL}_i}{\mathrm{NL_B}}. \tag{2}$$

Initial glass dissolution rate. The glass dissolution rate (g m^{-2} d^{-1}) is defined by the following expression:

$$r_{(i)} = \frac{\mathrm{dNL}_i}{\mathrm{d}t}. \tag{3}$$

2.5. STEM characterization of alteration products

Ultramicrotome cross-sections of the three altered glass monoliths prepared according to the technique described by Ehret et al. [19] were observed using a scanning transmission electron microscope (Philips CM 120) equipped with a semi-quantitative EDS X-ray analysis system (EDAX). Chemical determination of Si, O, Al, Fe, Zr, Na, Nd, Ni, Zn, Ca, P and Mo was performed with a 15 nm electron beam and an acceleration voltage of 100 kV, with the semi-quantitative results presented as element ratios. Only the changes in the Si/O ratio are discussed here, although the same results are obtained for the Si/Fe, Si/Zr and Si/Ce ratios.

3. Results

3.1. Preliminary open-system glass alteration

The solution analysis data are shown in Table 2. Under the test conditions, glass dissolution was practically congruent. Steady-state concentrations were reached for the analyzed elements after about 1 day; the solution pH remained stable at about 8.2. The mean glass dissolution rate was 0.54 g m^{-2} d^{-1}, a value very near the initial rate at the test temperature and pH. Advocat et al. [20] reported an initial rate of 1 g m^{-2} d^{-1} for the same glass composition at 90°C and pH 8, measured on monolithic test coupons for which the reactive surface area was assumed equal to the geometric surface area. Taking the surface roughness into account typically results in a difference by a factor of 2 [21].

The altered glass thickness after 7 days was estimated from NL(B) at 1.16 μm (Table 5). The silicon retention in the alteration products ranged from 5% to 10%, corresponding to the values measured by Advocat under initial rate conditions [20].

Table 2

Solution analysis data for the flowing experiment: concentrations C and normalized glass mass loss values NL calculated from Eq. (1); mean glass dissolution rate r (for $t = 1$ to 7 days) and standard deviation (S.D.); silicon retention factor f_{Si} in the alteration products calculated from Eq. (2)

t (days)	Flow rate (ml min^{-1})	pH at 90°C	C(Si) (mg l^{-1})	C(B) (mg l^{-1})	C(Na) (mg l^{-1})	C(Li) (mg l^{-1})	C(Al) (mg l^{-1})	C(Ca) (mg l^{-1})	NL(Si) (g m^{-2})	NL(B) (g m^{-2})	NL(Na) (g m^{-2})	r(B) (g m^{-2} d^{-1})	f_{Si}
0.25	1.44	7.95	1.05	0.18	0.77	0.04	0.18	0.26	0.05	0.04	0.11	0.18	−0.17
1	1.98	7.95	2.33	0.45	1.08	0.07	0.22	0.74	0.62	0.59	0.84	0.73	−0.06
2	1.27	8.25	2.09	0.47	1.03	0.08	0.20	0.53	0.72	0.79	1.03	0.20	0.09
3	1.22	8.36	2.87	0.67	1.17	0.11	0.30	0.38	1.43	1.62	1.69	0.83	0.12
4	1.18	8.52	3.03	0.71	1.28	0.13	0.28	0.55	1.94	2.22	2.38	0.60	0.13
7	1.08	8.25	2.93	0.64	1.29	0.11	0.29	0.67	3.00	3.18	3.84	0.32	0.06
Mean r(B)												0.54	
S.D.												0.28	

3.2. Static tests at $S/V = 500\ \mathrm{m}^{-1}$

The solution analysis data for the two static tests (ST1 and ST2) are indicated in Tables 3 and 4. The pH values for both tests were very similar, rising in a few days from the pH of pure water (about 6.5 at 90°C) to 8.9, then stabilizing at that value.

The alteration kinetics of the two glass specimens were very different, however, as shown by the normalized glass mass loss curves calculated from the boron concentrations (Fig. 1) and the variation of the alteration rates over time (Fig. 2). On completion of the test, the previously altered glass was 2.7 times as altered as the pristine glass. The differences were noted primarily between the 1st and 56th days (Fig. 2): the alteration rate for both specimens diminished from the initial rate r_0 to about $r_0/5$ during the first day, but subsequently diminished much more slowly for the previously altered glass than for the initially pristine specimen. The initial state of the glass (pristine or previously altered) thus affects the mechanism controlling the diminishing alteration rate. After 56 days, the alteration rates in both cases were less than 10^{-3} g m^{-2} d^{-1} (i.e. $r_0/1000$); the uncertainty on rates of such magnitude makes it impossible to identify any differences after 56 days.

The silicon concentrations were also very different in the two tests (Fig. 3). At the first sampling interval, the Si concentration was twice as high for the ST2 test as for ST1, as were the concentrations of the tracer elements (B, Na, Li). Between 1 and 56 days the Si concentrations rose more quickly in the ST1 test medium. The concentrations stabilized after 56 days in both cases; the Si concentrations at the end of the experiment were twice as high for the previously altered glass (ST1) as for the pristine glass (ST2).

The ultrafiltered 84-day solution samples showed no significant differences in the concentrations of the dissolved species (Tables 3 and 4), confirming the absence of colloids in the leachates.

3.3. Characterization of alteration films

Fig. 4(A) shows a cross-section through the alteration products formed during the flowing experiment. The gel is clearly visible, as are the surface precipitates forming a rather heterogeneous layer. The morphology of the precipitates is characteristic of rare earth phosphates and phyllosilicates – the two phases generally described in this region [3]. The gel thickness ranged from 0.5 to 1 μm, and the precipitated layer at the gel/solution interface was about 0.1 μm thick (Table 5). The thickness measured by STEM observation was appreciably less than that of the altered glass, suggesting that shrinkage of the alteration film occurred during drying. Localized analyses within the gel layer (Fig. 4(B)) show a

Table 3

Solution analysis data for static-mode experiment as $S/V = 500\ \mathrm{m^{-1}}$ with glass specimen ST1 (previously altered under flowing conditions): concentrations C and normalized glass mass loss values NL calculated from Eq. (1); silicon retention factor f_{Si} in the alteration products calculated from Eq. (2)

t (days)	pH at 90°C	C(Si) (mg l^{-1})	C(B) (mg l^{-1})	C(Na) (mg l^{-1})	C(Li) (mg l^{-1})	C(Al) (mg l^{-1})	C(Ca) (mg l^{-1})	NL(Si) (g m^{-2})	NL(B) (g m^{-2})	NL(Na) (g m^{-2})	NL(Li) (g m^{-2})	f_{Si}
0.17	8.25	4.5	1.2	2.4	0.2	0.5	1.04	0.04	0.05	0.07	0.03	0.23
1	8.65	18.8	6.4	10.3	1.3	1.4	1.07	0.17	0.29	0.28	0.28	0.40
7	8.81	39.9	16.5	25.3	3.3	1.5	1.32	0.36	0.73	0.67	0.69	0.50
14	8.85	53.5	25.7	39.7	5.0	1.3	1.23	0.48	1.13	1.04	1.05	0.57
28	8.95	62.2	31.5	48.6	6.1	1.2	0.83	0.55	1.36	1.25	1.24	0.60
56	8.92	66.1	31.5	48.5	6.3	1.2	0.92	0.58	1.34	1.23	1.26	0.57
84	8.95	68.4	32.3	48.1	6.2	1.3	0.89	0.58	1.34	1.19	1.22	0.57
84[a]	8.95	64.5	31.1	45.3	6.3	0.8	0.81	0.55	1.29	1.12	1.24	0.58

[a] Final test sample corresponds to ultrafiltered solution (10 000 Dalton).

Table 4

Solution analysis data for static-mode experiment as $S/V = 500\ \mathrm{m^{-1}}$ with pristine glass specimen ST2: concentrations C and normalized glass mass loss values NL calculated from Eq. (1); silicon retention factor f_{Si} in the alteration products calculated from Eq. (2)

t (days)	pH at 90°C	C(Si) (mg l^{-1})	C(B) (mg l^{-1})	C(Na) (mg l^{-1})	C(Li) (mg l^{-1})	C(Al) (mg l^{-1})	C(Ca) (mg l^{-1})	NL(Si) (g m^{-2})	NL(B) (g m^{-2})	NL(Na) (g m^{-2})	NL(Li) (g m^{-2})	f_{Si}
0.17	8.3	8.0	2.1	4.4	0.4	0.9	1.9	0.08	0.10	0.12	0.09	0.22
1	8.64–8.69	18.0	5.3	9.8	1.1	1.6	2.3	0.17	0.24	0.26	0.23	0.31
7	8.81	25.5	8.2	14.7	1.7	1.7	2.8	0.23	0.36	0.39	0.35	0.36
14	8.85	28.5	9.3	16.4	1.9	1.9	2.5	0.26	0.41	0.43	0.40	0.37
28	8.85	30.2	9.9	17.8	2.2	1.7	2.3	0.27	0.43	0.46	0.44	0.38
56	9.03	34.5	11.3	19.6	2.4	1.7	2.0	0.30	0.48	0.50	0.49	0.37
84	8.75	36.8	11.9	20.8	2.6	1.7	2.1	0.31	0.49	0.51	0.51	0.37
84[a]	8.75	34.6	11.4	19.7	2.6	1.1	1.8	0.29	0.47	0.49	0.50	0.38

[a] Final test sample corresponds to ultrafiltered solution (10 000 Dalton).

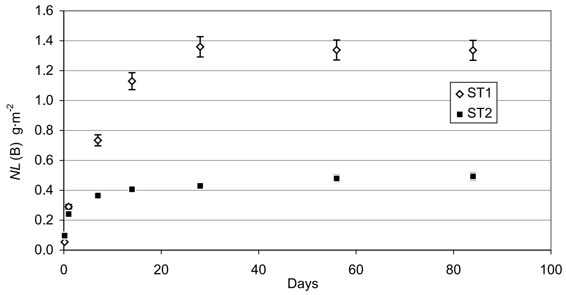

Fig. 1. Normalized glass mass losses calculated from boron concentrations in static tests ST1 (glass specimen previously altered under flowing conditions) and ST2 (pristine glass coupon) versus time at 90°C and $S/V = 500$ m^{-1}. Estimated uncertainty on normalized mass losses: 7%.

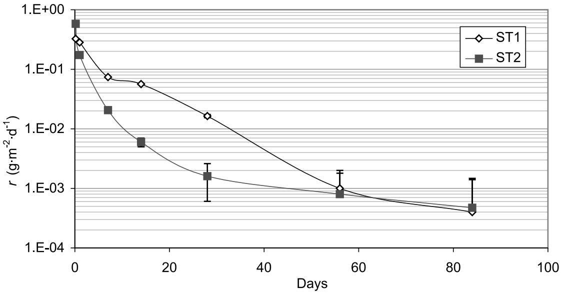

Fig. 2. Glass alteration rates in static tests ST1 (glass specimen previously altered under flowing conditions) and ST2 (pristine glass coupon) versus time at 90°C and $S/V = 500$ m^{-1}. Estimated uncertainty on alteration rates: 10^{-3} g m^{-2} d^{-1}.

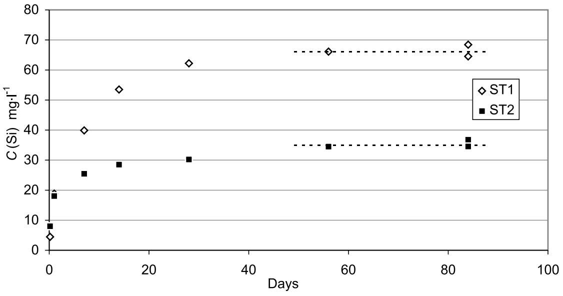

Fig. 3. Dissolved silicon concentrations in static tests ST1 (glass specimen previously altered under flowing conditions) and ST2 (pristine glass coupon) versus time at 90°C and $S/V = 500$ m^{-1}. Estimated uncertainty on concentrations: 3%.

constant Si/O ratio of 0.26 in the gel, appreciably below the corresponding ratio in the pristine glass (0.47).

Figs. 5 and 6 include images of the alteration products formed during the static tests. Fig. 5(A) (test ST2) shows a gel layer 150 ± 50 nm thick together with a rather heterogeneous phyllosilicate layer about 40 nm thick. The Si/O ratio in the gel (0.37) was constant at the same value as in the pristine glass (Fig. 5(B)), and significantly higher than in the flowing experiment, suggesting that the gel network formed during the static tests was probably better cross-linked than the network formed during alteration under flowing conditions.

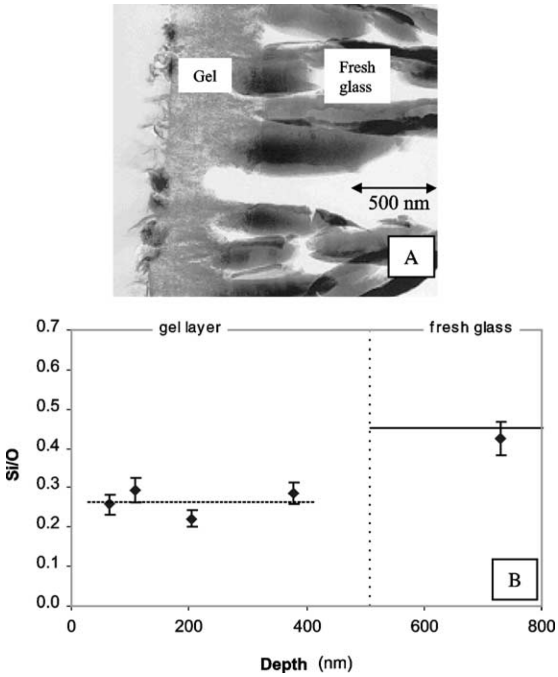

Fig. 4. STEM characterization of alteration film formed during flowing experiment. (A) Morphology of alteration film showing (left to right): secondary phases precipitated at gel/solution interface (rare earth phosphates and phyllosilicates), gel layer formed by recondensation of silicate species, and pristine glass splinters (due to ultramicrotome). (B) Localized chemical analyses in gel and pristine glass. Solid line corresponds to theoretical Si/O ratio in pristine glass; broken line is a visual aid for clarity.

Fig. 6(A) is a cross-section of the alteration products that formed on the specimen leached successively under flowing and static conditions. Two regions can be distinguished within the total gel layer about 1000 ± 200 nm thick: an inner region about 200 nm thick and an outer region about 800 nm thick. The outer region corresponds to the gel formed during the flowing experiment, while the inner region was formed during static leaching. As noted above, the thicknesses determined by STEM measurements were less than those determined from the boron concentrations (Table 5). The Si/O profile (Fig. 6(B)) indicates that this ratio gradually diminishes from the glass/gel interface, where it is the same as in the pristine glass (0.47), to the glass/solution interface, where it corresponds to the value measured in the gel formed under flowing conditions (0.26).

Table 5
Altered glass thicknesses determined from boron concentrations in solution, thickness of alteration films observed by STEM, and from measured specimen mass loss

Altered glass thickness (μm)	Dynamic test	Static test on previously altered glass (ST1)	Static test on pristine glass (ST2)
Solution analysis data			
Equivalent boron thickness	1.16	0.49 (+1.16)* = 1.65	0.18
STEM observation data			
Gel thickness	0.5–1	0.2–0.3 (+0.5–1)*	0.10–0.15
Precipitated thickness	≈0.1	≈0.15	≈0.04
Specimen mass loss data			
Gel thickness	1.0	1.5	Unmeasurable

* Gel previously formed under flowing conditions.

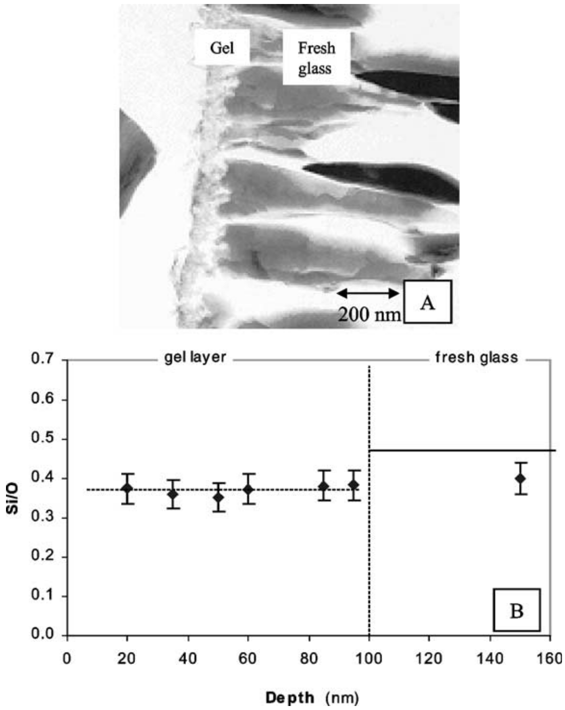

Fig. 5. STEM characterization of alteration film formed during static alteration of pristine glass specimen (ST2). (A) Morphology of alteration film showing (left to right): gel layer formed by recondensation of silicate species, and pristine glass splinters (due to ultramicrotome). (B) Localized chemical analyses in gel and pristine glass. Solid line corresponds to theoretical Si/O ratio in pristine glass; broken line is a visual aid for clarity.

The ST1 experiment thus did not yield the same Si/O ratio in the gel formed during the flowing alteration phase. The result indicates that a fraction of the silicon hydrolyzed during the static experiment was retained in the non-protective gel formed during the flowing experiment.

4. Discussion

4.1. Experimental findings

Analysis of the leachates from static test ST2 showed that between 0 and 0.17 day alteration occurred at the initial rate of 0.5 g m^{-2} d^{-1} measured during the dynamic test. Over the same time interval, the previously altered glass dissolved at only half this rate. This behavior could be attributable to a partial diffusion barrier due to the preexisting gel layer. This behavior was transient, however, and after 1 day the trend was reversed, showing that a different limiting mechanism was involved at this stage of reaction progress.

During the time period corresponding to the transition from the initial rate to the final rate characteristic of a steady-state silicon concentration, static tests ST1 and ST2 show that the glass alteration kinetics were strongly influenced by the presence of the gel formed during the flowing experiment (Fig. 2). The silicon fractions retained in the two types of gel (calculated from the differences between the boron and silicon flows) were not the same (Tables 3 and 4), but this calculation provides no indication of the silicon distribution in the gel – and this is an essential point.

The leachate analysis results show that the steady-state silicon concentrations were also dependent on the initial system conditions. This observation can be interpreted only by considering that the steady-state dissolved silicon concentrations depend on the nature of the gel – i.e. it is not an inherent glass property. This is equivalent to asserting that the steady-state value does not correspond to the glass solubility, and that the difference between the silicon concentration at any given instant and the steady-state concentration is therefore not representative of the chemical affinity of the glass dissolution reaction. From this standpoint, these observations corroborate the results of other recent works in this area [5,7].

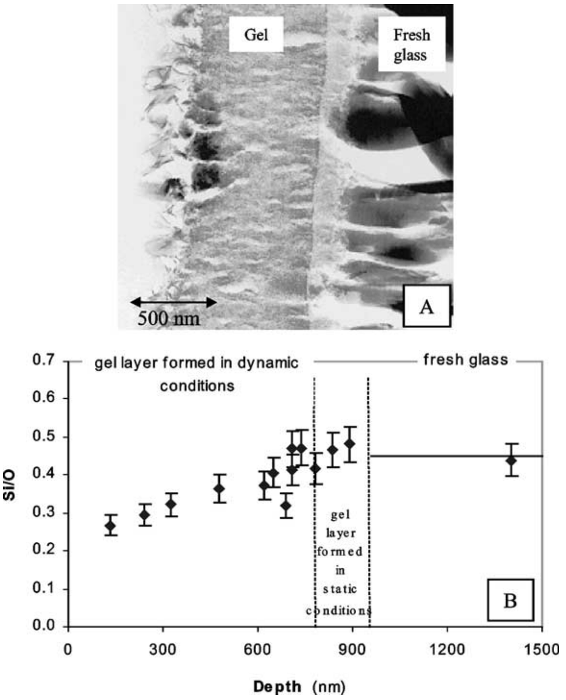

Fig. 6. STEM characterization of alteration film formed by flowing and static alteration of glass specimen (ST1). (A) Morphology of alteration film showing (left to right): secondary phases precipitated at gel/solution interface (rare earth phosphates and phyllosilicates), gel layer formed by recondensation of silicate species (comprising gel formed during flowing experiment and gel formed during static test), and pristine glass splinters (due to ultramicrotome). (B) Localized chemical analyses in gel and pristine glass. Solid line corresponds to theoretical Si/O ratio in pristine glass; broken line is a visual aid for clarity.

Although the silicon concentration in solution is not the parameter controlling the glass alteration kinetics, its role as a gel forming agent is fundamental. SON 68 glass alteration experiments in clay with strong complexation properties [9] have shown that the presence of silicon in the gel was necessary to constitute an effective diffusion barrier between the glass and solution. The presence of insoluble elements such as Zr or the rare earth elements favors cross-linkage in the gel and enhances its protective properties [5], but this is possible only in a silicate network formed by recondensation of hydrolyzed silicon.

4.2. STEM examination results

STEM observation of the alteration films formed during static experiments ST1 and ST2 showed that a fraction of the silicon from the glass that was hydrolyzed during static alteration (ST1) migrated into the gel previously formed during the flowing experiment. The fact that Si/O ratios exceeding 0.25 were measured within the outer portion of the gel on this sample confirms that silicon migrated through the entire non-protective gel layer. This further suggests that a fraction of the silicon hydrolyzed during the static test migrated completely into solution, and would account for the higher dissolved Si concentrations measured in test ST1 than in test ST2. Similar results were obtained for the Si/Fe, Si/Zr and Si/Nd ratios.

These observations, however, do not account for the fact that the glass was 2.7 times as altered in test ST1 as in test ST2.

The preceding observations indicate that silicon recondensation was relatively uniform (i.e. with a long diffusion distance before recondensation, compared with the thickness of the alteration film) rather than localized. The alteration products (non-protective gel and/or phyllosilicates) that formed under flowing conditions thus exhibited the behavior of a silica pump comparable to the phenomena observed when glass is altered in the presence of clay [9]. Saturation of the gel thus appears to be indispensable before it can become protective, and limits the kinetics of glass network dissolution.

4.3. Gel density

Assuming that glass dissolution is a constant-volume process, and considering that in experiment ST1 the gel formed under flowing conditions was not dissolved during the static phase, a material balance based on the silicon concentrations in the three gels in this series of experiments yields the following results (the gel thicknesses indicated are based on the observed normalized boron mass losses):

- On completion of the flowing experiment: $d_{\mathrm{Si}} = 0.7$ Si atom/nm^3 of gel.
- After static leaching of the previously altered specimen (ST1): $d_{\mathrm{Si}} = 2.6$ Si atoms/nm^3 of gel on average over the total thickness, taking into account the additional silicon corresponding to the dynamic and subsequent static alteration phases.
- After static leaching of the pristine glass specimen (ST2): $d_{\mathrm{Si}} = 4.6$ Si atoms/nm^3 of gel.

The silicon profile in the gel on specimen ST1 reveals that near the glass/gel interface the Si/O ratio was the same as the value measured in the pristine glass, as in the case of specimen ST2. It may thus be assumed that the local silicon density near the reaction interface is 4.6 Si atoms/nm^3 of gel, as in the pristine glass. Moreover, the outer portion of the gel was not enriched in Si by comparison with the gel formed only during prior alteration under flowing conditions (Figs. 4 and 6). It can therefore also be assumed that the local silicon density in the outermost portion of the gel is 0.7 Si atom/nm^3 of gel, as in the gel formed under flowing conditions. This implies a density gradient between the reaction interface region and the outer portion of the gel. The distribution of the total quantity of silicon retained throughout the gel was calculated assuming a linear density gradient between the upper limit (4.6 Si atoms/nm^3 of gel) and the lower limit (0.7 Si atom/nm^3 of gel); the upper limit was reached to a depth of no more than 300 nm near the interface, and that at least 150 nm on the outer region of the gel showed no Si enrichment.

These results suggest the existence of a critical density above which the transport of glass species is sharply reduced, although further work will be necessary to substantiate this hypothesis. The critical density must be associated with a characteristic thickness to qualify the gel as 'protective'. In future work, we will focus on determining the possible relation between the protective gel density and thickness by examining alteration films formed at different stages of reaction progress.

4.4. Protective gel formation conditions

For many years, it has been observed that increasing the S/V ratio of static alteration experiments tends to increase the solution pH, increase the dissolved silicon concentration, and diminish the altered glass thickness after a given time interval [22,23]: the higher the S/V ratio, the faster the alteration rate diminishes. The classic interpretation of this observation is in terms of saturation. Increasing the S/V ratio allows solution saturation conditions to be reached sooner; hence the rate diminishes more quickly at higher S/V ratios. It is also acknowledged that a higher pH results in a greater apparent silica solubility of the glass. However, this interpretation breaks down in the case of a pristine glass specimen that dissolves at its initial rate r_0 as long as a protective gel has not been formed [5,7].

In the light of this work, the notion of solution saturation with respect to silica must be considered prudently, inasmuch as it apparently depends on the nature of the gel and thus on the specimen history [24]. Experimental work carried out since 1990 on the effects of the glass composition has led some authors to suggest that the protective properties of the gel could increase with the S/V ratio [25]. The interpretation of our experimental data confirms this hypothesis and may explain the mechanisms involved.

The gel is formed by recondensation of hydrolyzed species. The recondensation rate depends primarily on the ratio between the number of recondensation sites and the concentration of species liable to recondense. When a pristine glass specimen is placed in pure water, the recondensation rate is low: the gel formed in the early stages of the reaction contains little silicon and its protective properties are very limited. Two hypotheses may be postulated at this point:

1. the gel (or a fraction of the gel) must be saturated with respect to silicon in order to become protective;
2. an unsaturated gel (or phyllosilicate layer) constitutes a silicon pump.

According to these hypotheses, the glass quantity that must be dissolved to saturate the gel depends on the mass of non-protective gel – which is inversely proportional to the S/V ratio. The lower the S/V ratio, the greater the mass of unsaturated gel; this implies a major silica pump effect, hence a delay in the formation of a sufficient thickness of saturated, protective gel. The required minimum density necessary to obtain a protective gel thus accounts for the effect of the S/V ratio observed in the case of nuclear glasses.

It is still remains to be understood why the non-protective gel formed during the flowing experiment constitutes a pump for the silicon hydrolyzed during the static test. Identification of the elementary mechanisms involved in this effect will require additional work, notably to determine whether the delay in reaching saturation conditions is related to restructuring of the gel or to the growth of secondary crystallized phases.

5. Conclusions

This study confirms that the notion of solution saturation with respect to silicon is not an inherent glass characteristic, since the steady-state concentrations depend on the gel formation conditions – and in particular on the capacity of the medium to provide or remove silicon. The degree of gel protection also depends on the experimental conditions. Nevertheless, it appears that the gel must reach a given silicon concentration before it becomes protective. The observations corroborating this hypothesis are consistent with the effects of the S/V ratio on the alteration kinetics of nuclear glass.

Acknowledgements

The authors are grateful to Ms Labruquère of the University of Poitiers (France) for the STEM examinations.

References

[1] European Standard ENV 12920, 1997.
[2] E.Y. Vernaz, J.L. Dussossoy, Appl. Geochem. (Suppl. 1) (1992) 13.
[3] J.L. Noguès, E.Y. Vernaz, N. Jacquet-Francillon, Mater. Res. Soc. Symp. Proc. 44 (1985) 89.
[4] Z. Bocksay, G. Bouquet, S. Dobos, Phys. Chem. Glasses 9 (1968) 69.

[5] C. Jégou, PhD thesis, University of Montpellier, France, 1998, p. 207.

[6] C. Jégou, S. Gin, E.Y. Vernaz, F. Larché, in: International Congress on Glass XVIII, American Ceramic Society, July 1998, 1999.

[7] S. Gin, C. Jégou, E.Y. Vernaz, F. Larché, in: International Congress on Glass XVIII, American Ceramic Society, July 1998, 1999.

[8] S. Gin, C. Jégou, E.Y. Vernaz, Appl. Geochem. 15 (2000) 1505.

[9] S. Gin, P. Jollivet , J.P. Mestre, M. Jullien, C. Pozo, Appl. Geochem., 2001, accepted.

[10] C. Jégou, S. Gin, F. Larché, J. Nucl. Mater. 280 (2000) 216.

[11] J.P. Jolivet, De la solution à l'oxyde, Inter Ed./CNRS Ed., 1994.

[12] S. Ricol, PhD thesis, Université Pierre et Marie Curie (Paris VI), France, 1995.

[13] O. Deruelle, O. Spalla, P. Barboux, J. Lambard, J. Non-Cryst. Solids 261 (2000) 237.

[14] E.Y. Vernaz, N. Godon, Mater. Res. Soc. Symp. Proc. 257 (1992) 37.

[15] O. Ménard, T. Advocat, J.P. Ambrosi, A. Michard, Appl. Geochem. 13 (1998) 105.

[16] L.A. Chick, L.R. Pederson, Mater. Res. Soc. Symp. Proc. 26 (1984) 635.

[17] F. Pacaud, N. Jacquet-Francillon, A. Terki, C. Fillet, Mater. Res. Soc. Symp. Proc. 127 (1988) 105.

[18] B.E. Scheetz, W.P. Freeborn, C. Anderson, M. Zolensky, W.B. White, Mater. Res. Soc. Symp. Proc. 44 (1985) 129.

[19] G. Ehret, J.L. Crovisier, J.P. Eberhart, J. Non-Cryst. Solids 86 (1986) 72.

[20] T. Advocat, J.L. Crovisier, E.Y. Vernaz, G. Ehret, H. Charpentier, Mater. Res. Soc. Symp. Proc. 212 (1991) 57.

[21] M. Jaycock, G.D. Parfitt, in: Chemistry of Interfaces, Ellis Harwood, Chichester, UK, 1981.

[22] R.B. Agida, E.P. Akomer, D.E. Clark, Mater. Res. Soc. Symp. Proc. 44 (1985) 45.

[23] W.L. Ebert, J.J. Mazer, Mater. Res. Soc. Symp. Proc. 333 (1994) 27.

[24] E.Y. Vernaz, S. Gin, these Proceedings, 2000.

[25] X. Feng, I.L. Pegg, Y. Guo, A.A. Barkatt, P.B. Macedo, Mater. Res. Soc. Symp. Proc. 176 (1990) 383.